SUPPORTING INFORMATION

Mathematical modeling

Host landscape

The spatial distribution of host species across California susceptible to infection by *Phytophthora ramorum* was mapped as described in Meentemeyer *et al.* (1), leading to a finely-resolved statewide map of the availability of host (Fig. S2A). Each of the approximately 15.4 million cells that was used to cover California with a 3656 x 4218 rectangular grid of 250 x 250m cells was assigned a number of "host units" that could potentially become infected. Differences in the host index h_i in each cell i integrate differences between cells in terms of the local coverage, susceptibility and infectivity of *P. ramorum* host species, and so allow for different rates of within-cell pathogen bulk-up and between-cell spread. The maximum number of host units that can be contained in a single cell is $N^{max} = 100$. A total of approximately 1.35 million cells across California have $h_i > 0$.

Forest type masks

Following Meentemeyer *et al.* (1), each cell is also associated with one of two forest type masks (Fig. S2B), f_i, that distinguishes cells dominated by redwood-tanoak (f_i = R) from mixed-evergreen forests, typically dominated by coast live oak and bay laurel (with

f_i = M). The forest type mask controls the weeks within each year in which each cell is infectious and susceptible. These date ranges were changed from those reported in (1) in the light of new data (2). Infection by and of cells of type R can only occur between January 1st and July 15th (i.e. weeks 1 to 28 of the year), whereas the corresponding restriction in cells of type M is from February 15th to July 15th (i.e. weeks 7 to 28 of the year). The change in date range affects the number of weeks per year in which infected cells can transmit the pathogen, and therefore required recalibration of β, the rate of infection in the model (see below). In our update to the original model to include pathogen detection, the forest type mask also affects the rate at which symptoms emerge within a cell (see below).

Environmental conditions

Within- and between-cell infection dynamics depend on environmental conditions, since sporulation and transmission of *P. ramorum* are sensitive to temperature and precipitation. We therefore mapped time-dependent temperature and moisture suitability indices, calculated as described in (1), at the 250m x 250m scale on the weekly time-step used by our model. These values are used in the model to modulate the rate of spore production and infection, as described in (1).

Yearly samples of sequences of weeks from these spatio-temporal patterns in environmental drivers of infection were used to forecast future weather patterns when necessary for forward simulation, again as is fully described in (1). This allowed us to

associate each cell i with two time-dependent pathogen suitability indices in week t over the any range of dates: c_{it}, the temperature index, and m_{it} the moisture index, both on a [0,1] scale. These environmental drivers affect the sporulation rate and the probability of infection, as described below.

Epidemiological transitions

Individual host units in the i^{th} cell at time t can be in one of three states, susceptible (s_{it}), infected (i_{it}) or removed (r_{it}), with $s_{it} + i_{it} + r_{it} = h_i$. Each cell must also be in one of the following six mutually-exclusive epidemiological classes, driven by the cell's infection history, whether or not is has been affected by management, and the current state of the host units it contains (*cf.* Fig. 1A in the main text)

- (S)usceptible. Not infected or affected by control.
- (C)ryptic. Infected but too recently to yet show symptoms.
- (I)nfected. Infected and showing detectable symptoms.
- (D)etected. Infected and detected but not yet controlled.
- (T)reated. Never been infected, but has previously had host units removed due to control triggered by an infected neighbor.
- (R)emoved. Contained infected host units, but since then has had all infected host units removed due to control.

Transitions of host units between states, and of cells between epidemiological classes, occur on a weekly time step.

Infection

Infection is caused by transmission of the pathogen from cells containing infected host units to cells containing susceptible host units (note that self-infection within the same cell is possible). Local and long-distance spread are accounted for via a mixture of Cauchy kernels (see below), and – as in the Meentemeyer *et al.* model (1) – the rate of infection is moderated by the dominant forest type and by the environmental conditions in both donor and recipient cells. We assume infected cells are immediately infectious, since the latent period of *P. ramorum* is short for at least some species within its host range (3).

Infected host units potentially produce new infections on a weekly time-step. The maximum number of mean infections arising from site i in week t is given by $\psi_{it} = \beta\chi_t(f_i)m_{it}c_{it}i_{it}$, in which

- f_i is the forest type of cell i;
- $\chi_t(f_i)$ is a seasonal indictor variable controlling whether infection by cells of forest type f_i is possible in week t;
- i_{it} is the number of infected host units in cell i in week t;
- the rate of infection, β, is the mean number of new infections that could be produced by a single infected host unit if the environmental conditions were to be perfectly conducive and if all challenges were to lead to infection of a susceptible host unit;

- the spatio-temporal environmental suitability indices, c_{it}, and m_{it}, are as described above.

In each week, *t*, each infected cell *i* produces a Poisson distributed (mean ψ_{it}) number of potential challenges. Cells that are challenged for potential infection are located by sampling a dispersal distance from our dispersal kernel, $K(d;\alpha_1,\alpha_2,\gamma)$ (see below), and finding the cell *j* that contains a point at that distance from the center of cell *i* on a random angle in [0, 2π). The challenged cell can be the same as the infected cell, i.e. *j* = *i*, and so self-infection is possible. If there is/are susceptible host unit(s) in the challenged cell, *j*, it then becomes infected according to a single Bernoulli trial with probability of success equal to $\chi_t(f_j)m_{jt}c_{jt}s_{it}/N^{\max}$. If infection occurs in a cell that currently contains no infected host units (i.e. has i_{it} = 0 directly before it becomes infected), then the cell enters the epidemiological class C (i.e. the cell becomes cryptically infected). We note this transition can occur not only for cells in class S, but also for cells in classes T and R (see below).

Dispersal kernel

Our dispersal kernel, $K(d;\alpha_1,\alpha_2,\gamma)$, accounts for two scales of pathogen dispersal via a mixture of Cauchy kernels

$$K(d;\alpha_1,\alpha_2,\gamma) \propto \gamma\left(1+(d/\alpha_1)^2\right)^{-1}+(1-\gamma)\left(1+(d/\alpha_2)^2\right)^{-1}. \quad (1)$$

The parameter α_1 controls the scale of short-range dispersal, α_2 controls the scale of long-range dispersal, and γ controls the proportion of short-range infection. We used

the values of α_1, α_2 and γ reported in (1), which were originally determined by fitting to survey data from two spatial scales via MCMC methods: the short-range component using mortality data from the spatially-isolated outbreak in Humboldt county and the long-range component from statewide survey data.

Recalibration of the infection rate

We use the same host index, forest type masks, environmental drivers, and dispersal kernel as in (1). Since the extensions to the model to account for detection and control do not affect the rate of spread when management is not attempted, these did not need to be accounted for by any changes to the model parameters. However, the change to the date ranges in which cells of different forest type masks are infectious and can be infected leads to a different overall spread rate, effectively by re-scaling time, and the rate of infection, β, was therefore recalibrated to reflect this.

We updated the value of β by a line search, calibrating the results of the model using the new sporulation dates against the results as previously reported in (1). In particular, we performed 1,000 replicate simulations of the model between 1990 and 2030 using the original date ranges for sporulation with the previously-reported value β = 4.4wk^{-1} (1), and calculated the average area infected at the end of each year *y*, $A^{orig}(y)$. We then simulated the model using the updated dates controlling sporulation for a range of values of β, calculating the average area infected at the end of year *y*, $A_{\beta}^{new}(y)$, again for

1,000 replicate simulations for each value of β. We then used the sum of squared differences

$$E_{\beta}^{2} = \sum_{y=1990}^{2030} \left(A^{orig}(y) - A_{\beta}^{new}(y) \right)^{2}, \quad (2)$$

as a measure of the difference between the results using the two date ranges for each value of β as used in the model with the updated date ranges, and selected the updated value β = 4.55wk^{-1} that minimized E_{β}^{2} (Fig. S3). This value of β was used for all simulations presented in the paper.

Hazard map

One of the ways in which control can be targeted is to focus on locations with high potential for local disease amplification and secondary spread via the so-called "hazard map". This is a map showing the result of simulating a hypothetical epidemic by artificially seeding the model with a single isolated infection in an otherwise totally susceptible landscape in which all hosts are at the density implied by our mapping procedure (see above), and averaging the number of infected cells after a fixed time (5 years) over a number of independent runs of the model. The hazard map is therefore a spatially-resolved proxy for the basic reproductive number (R_0) that accounts for local pathogen bulk-up within a fixed carrying capacity, connectivity of host populations and environmental conditions. The hazard map reported in (1) was obtained by calculating the value of the hazard for 1,000 randomly chosen locations across the state, and then using ordinary kriging to spatially-interpolate values at other locations. Here we instead calculate the hazard for every cell over the entire landscape with $h_i > 0$. This reveals

significant fine-scale detail omitted from the version presented in the earlier paper (Figs. S2C and D).

Emergence and detection of symptoms

We account for pre-symptomatic cryptic transmission (4) by including an average delay of three or five years between infection and the emergence of symptoms, depending on host species. We assume cells containing symptomatic hosts can be detected by a statewide program of monitoring via aerial surveying followed by ground inspection. Symptoms therefore correspond to crown mortality observable by aerial surveying. We model symptom emergence as potentially occurring continuously throughout the year, with cells in class C entering class I according to a single Bernoulli trial once per week, with probability of success θ per week, where $\theta = 1/260 wk^{-1}$ for cells of type M, and $\theta = 1/156 wk^{-1}$ for cells of type R. These values are parameterized from field-measured periods of sporulation and rates of infection and of mortality for infected trees (2, 5). The distribution of cryptic periods is therefore geometric, and for simplicity it is assumed to be independent of the number of infected host units within the cell.

In the model, detection occurs synchronously across the entire state in early June. Cells in class I are potentially detected according to a single Bernoulli trial with probability of success, $p = 0.8$, and cells that are detected (and so enter class D) are added to the current list of sites known to contain infection to potentially be controlled later. In the absence of data that would allow a more complex model of detection to be

parameterized, we assume detection is also independent of the number of infected host units within a cell.

Re-establishment of susceptible hosts

Cells that have ever had any host units removed by control (i.e. have $r_{it} > 0$) are subject to re-establishment of susceptible hosts, up to the limit of the original carrying capacity h_i (which we assume is constant over the timescale of our study). We do not model disease-induced death of host trees, because re-sprouting is prolific from root-stock that survives after the death of the crown (6), and because re-sprouting is adequate to maintain pathogen populations (7). Re-establishment after treatment occurs once per year for computational convenience, and is done by setting a binomially-distributed number, Bin(r_{it},ρ), of the r_{it} removed host units in cell i to revert to be susceptible directly before the first week of each year, where $\rho = 0.2yr^{-1}$ is the yearly re-establishment rate. This corresponds to the average combined time required for re-establishment of basal sprouts in the forest understory canopy and re-infection in field experiments designed to eradicate the pathogen from an isolated outbreak where inoculum pressure was sustained by nearby untreated locations (8). The time-scale is also consistent with those reported for re-infection of basal sprouts following above ground mortality of host trees during fire (7).

Control

We model treatment as occurring in mid-November, synchronously across the state, and assume it removes all *P. ramorum* susceptible and infected hosts within a certain radius of detected infection. However, budgetary constraints mean that, in general, treatment of all detected infection foci would be impossible. Cells containing currently uncontrolled detected infection are sorted by treatment priority (see below), and as many as possible are considered as treatment foci until the budget is exhausted. Both susceptible and infected host units are removed from cells including and surrounding the focal cell up to a certain control radius, L, setting the proportion q of host units to remove according to the fraction of the cell in question that lies within a circle of radius L centered on the focal cell (Fig. S4). If $q = 1$, all host units are simply removed from the cell at the time of control. For any cells with $q < 1$, removal of host units depends on whether the cell in question has previously had any host units removed. If no host units have previously been removed, then individual host units are removed according to a series of Bernoulli trials each with probability of success q, and where there is no distinction in the probability of removal between susceptible and infected host units (i.e. infected host units are not removed preferentially). However, if the cell already contains removed host units, we calculate the proportion that has not yet been removed in cell j, $z_j = (s_{jt} + i_{jt})/h_j$, and then remove these remaining host units according to a series of individual Bernoulli trials each with probability of success q/z_j (or simply remove all host units from the cell if this ratio is greater than one). When treatment of all cells within radius L of a focal cell is complete, the focal cell is removed from the detected list (although it can be added back into the list on a subsequent survey if by then symptomatic infected host units are detected within the cell). Treated cells which

no longer contain infected host units (i.e. have i_{it} = 0) enter either the T or R class depending on their infection status before treatment (*cf.* Fig. 1A in the main text). In either case, and as described above, any later re-infection of any cell that has previously been controlled causes it to enter the cryptically-infected (C) class.

Prioritizing cells for treatment

Before each round of control, each cell j in the detected list is given a control priority score σ_j. The host, hazard, infected and susceptible strategies calculate control priorities over the local neighborhood, Ω_j, which based on exploratory work we defined to be a circle of radius Q = 2km centered on cell j. Scores are calculated as follows, where f_k is the fraction of cell k in the neighborhood Ω_j, and where the epidemiological class of cell i in week t is τ_{it}.

- Random. Do not prioritize (the default) and set σ_j to be a random number.
- Host. Prioritize cells in areas where there is a large amount of *P. ramorum* host

$$\sigma_j = \sum_{k \in \Omega_j} f_k (s_k + i_k).$$

- Hazard. Prioritize cells in areas where there is a high hazard (i.e. potential for rapid local spread, analogous to local R_0)

$$\sigma_j = \sum_{k \in \Omega_j} f_k \log(H_k),$$

where H_k is the hazard of cell k.

- Wave-front. Prioritize cells that are on or ahead of the spreading wave of infection, which here, after exploratory work indicating more complex methods for identifying the wave-front did not lead to improved performance, we conveniently characterize by setting the cell's score to be proportional to its distance north.

- Infected. Prioritize cells in areas where a large proportion of host is currently infected

$$\sigma_j = \sum_{k \in \Omega_j, \tau_{kt} \in \{I,D\}} f_k \left(\frac{i_{kt}}{h_k} \right).$$

  Cryptically-infected cells $\tau_{kt} = C$ do not contribute to this score, since they are not visibly infected.

- Susceptible. Prioritize cells in areas where a large proportion of host remains uninfected

$$\sigma_j = \sum_{k \in \Omega_j, \tau_{kt} \in \{S,I,D,R,T\}} f_k \left(\frac{s_{kt}}{h_k} \right) + \sum_{k \in \Omega_j, \tau_{kt} \in \{C\}} f_k \left(\frac{s_{kt} + i_{kt}}{h_k} \right).$$

  The calculation is deliberately adjusted to account for cryptically-infected cells, since in practice the infected hosts they contain would erroneously be assumed to be susceptible.

Before each round of control, the list of all cells known to currently contain uncontrolled infection is sorted by the control priority score, and control proceeds by treating in and around each cell in this sorted list until any budgetary constraint is exceeded (or until the entire list has been treated).

Budget

The budget for treatment is specified as a total area C km^2 that can be removed per year and by default any unused budget is carried over between years. If treatment removes c_j from the carrying capacity of h_j host units in cell j, this costs the equivalent of removing (1/16)(c_j/h_j) km^2 of host (since cells are 250m x 250m). Treatment stops after control in the first cell in which the budget is exceeded, with any focal cells around which control has not been completed remaining in the detected list for potential treatment in subsequent years. In the part of the work that corresponds to budgets that change over time (Fig. S1A), we assume that the amount that is added to the area that can be treated in year y for a program of control starting in year T_0 is $C(y) = C_0\alpha^{y-T_0}$. The initial budget, C_0, is chosen to ensure that a constant maximum amount is spent by the end of the period of interest, T_e = 2030, for all values of α, i.e.

$$C_0 = \frac{(1-\alpha)C(T_e - T_0 + 1)}{1-\alpha^{T_e - T_0 + 1}}.$$

A geometric progression was chosen for $C(y)$ to allow for treatment budgets that vary over time, while allowing normalization to the same total amount of control over a fixed time horizon, in a simple one-parameter model.

Estimating the cost of control

In the main paper, we assert that treating 200km^2/yr would cost at least 100 million USD/yr. There are two sources supporting this estimate. Kanaskie *et al.* (9) report a

cumulative cost of 7.5 million USD since 2001 for eradication treatments (felling and burning all *P. ramorum* host plants) on 3,000 acres of land in Oregon, corresponding to a cost of 2,500 USD per acre, or approximately 617,500 USD per km^2, and so 123.5 million USD/yr to treat 200km^2/yr. In California, exact expenditures for those small-scale management interventions that have been attempted (e.g. removal of hosts in the Jay Smith State Park) have not been reported. However, Valachovic *et al.* (10) estimate costs of 4,940-8,645 USD per hectare for treatment involving manual removal by chainsaw and pile burning of branches and foliage of all bay and tanoak with subsequent under-burning to remove inoculum on private lands, corresponding to between 494,000 USD and 864,500 USD per km^2. The lowest end of this range corresponds to a cost of 98.8 million USD/yr to remove 200km^2/yr. Both these previously-reported estimates are therefore consistent with our assertion in the main text that treatments would require a direct cost of at least 100 million USD per year. However, the additional costs of environmental compliance, potential for treating in remote areas with limited access, and other logistical challenges which have increased the per unit area cost in these management efforts suggest the actual cost of treating 200km^2 annually could in fact be as high as 222 million USD per year (4,500 USD per acre).

Balancing the costs of detection and treatment.

When examining the trade-off between spending on pathogen detection and treatment (Fig. S1B), we assume the area added to the control budget per year, C, is a linear function of the detection probability, p, with $C = C_{\max}\left(1 - p / p_{\max}\right)$, and where $C_{\max}$ and

p_{max} are the maximum area that can be treated when the entire budget is spent on treatment, and the maximum probability of detection when the entire budget is spent on disease survey, respectively. This is a proxy for a spatially-uniform survey that examines progressively fewer cells as the budget for detection is decreased.

Running the model and model outputs

The model is initiated as described in (1), and is seeded with a single infected host unit in each of three locations of hypothesized introduction in the San Francisco Bay Area in 1990. We perform a large number, typically N = 10,000, independent simulations per set of parameters we consider. Risk maps show the average infection risk over N replicate model simulations, where the infection risk for cell i at time t, ζ_{it}, is calculated as $\zeta_{it} = \frac{1}{N}\sum_{j=1}^{N}\left(i_{it}^{j} + r_{it}^{j}\right)$, in which i_{it}^{j} is the number of infected host units, and r_{it}^{j} is the number of removed host units, both taken in cell i in simulation run j at time t.

Additional results

Animations showing the risk of spread over time

Movie 1 shows the statewide evolution of the infection risk over time when there is no control (*cf.* Figs. 1B and 1C in the main text), and the risk when controlling an area of 200km^2/yr starting in 2014 is shown in Movie 2 (random selection of sites for treatment from the detected list; control radius = 375m; cf. Figs. 2A – 2C in the main text). Maps

showing changes in the risk over time using each of the six strategies for spatially-targeted control starting in 2002 and that can control up to 50km^2/yr are in Movies 3 to 8, where each strategy is shown using the control radius that optimizes its median performance (*cf.* Fig. 5A in the main text).

Additional disease progress curves for different starting years and budgets

Additional detail for a selection of the results shown in Fig. 3 in the main text are given in Figs. S5 and S6. These figures show disease progress curves (Fig. S5) and the amount of control performed over time (Fig. S6) for a selection of control budgets and years in which control is started.

Optimizing the spatial deployment of control

Additional disease progress curves showing the area lost over time for the spatially-optimized control strategies are given in Fig. S7 (*cf*. Fig 5 in the main text which shows only the area lost in 2030: here full disease progress curves are shown for a number of combinations of control strategy x control budget x year of starting control).

Fig. S8 shows a pair of disease progress curves for the spread of disease until 2050, comparing performance when not controlling vs. controlling using the wave-front strategy starting in 2014 with budget for control up to 50km^2/yr. The time at which 14,000km^2 is lost is marked by the black line. This supports our statement in the main paper that the wave-front strategy with a budget for control of up to 50km^2/yr does not

lead to effective control starting in 2014, but instead merely acts to delay the epidemic by approximately seven years.

Foci first control

As was described in the main text, by default control takes elements of the list of cells known to contain infection in order of control priority, σ, controlling cells within the control radius *L* of each cell in the list in turn, stopping as soon as the budget is exhausted. However, we also considered a two-pass "foci first" control strategy, in which as many as possible of the detected cells are controlled first, and then control around each detected cell in a neighborhood occurs only if there is budget remaining. We illustrate the difference in implementation via a schematic showing an example on a simple host landscape (Fig. S9).

The intuition underlying testing this strategy is that it potentially mitigates for a limited budget by targeting control more effectively in cells that are definitely known to contain infection. We tested by comparing performance of the default "treat first" vs. the "foci first" implementation of all six strategies for prioritizing where to treat, for management starting in 2002 which was able to control up to 50km^2/yr, with each strategy tested at its optimal radius as reported in the main text. In general, treating the foci first makes control strategies that would otherwise perform poorly more effective, but makes control strategies that effectively identify better cells to prioritize for treatment work less well (Fig. S10). However, the relative ordering of the different strategies is unaffected, and

the differences in control performance between the two implementations of each prioritization were relatively small.

REFERENCES

1. Meentemeyer R, et al. (2011) Epidemiological modeling of invasion in heterogeneous landscapes: spread of sudden oak death in California (1990-2030). *Ecosphere* 2:art17.

2. Davidson JM, Patterson HA, Wickland AC, Fichtner EJ, Rizzo DM (2011) Forest type influences transmission of Phytophthora ramorum in California oak woodlands. *Phytopathology* 101:492–501.

3. Rizzo D, Garbelotto M, Hansen E (2005) Phytophthora ramorum: Integrative research and management of an emerging pathogen in California and Oregon forests. *Annu Rev Phytopathol* 43:309–335.

4. Filipe JAN, et al. (2012) Landscape epidemiology and control of pathogens with cryptic and long-distance dispersal: sudden oak death in northern Californian forests. *PLOS Comput Biol* 8:e1002328.

5. Cobb RC, Filipe JAN, Meentemeyer RK, Gilligan CA, Rizzo DM (2012) Ecosystem transformation by emerging infectious disease: loss of large tanoak from California forests. *J Ecol* 100(3):712–722.

6. Cobb R, Meentemeyer R, Rizzo D (2010) Apparent competition in canopy trees determined by pathogen transmission rather than susceptibility. *Ecology* 91:327–333.

7. Beh M, Metz M, Frangioso K, Rizzo D (2012) The key host for an invasive forest pathogen also facilitates the pathogen's survival of wildfire in California forests. *New Phytol*:1145–1154.

8. Valachovic Y, Quinn-Davidson L, Lee C, Goldsworthy E, Cannon P (2013) Novel approaches to SOD management in California wildlands: a case study of eradication and collaboration in Redwood Valley. *Proc Sudd Oak Death Fifth Sci Symp*, p 99.

9. Kanaskie A, et al. (2011) Detection and eradication of Phytophthora ramorum from Oregon forests, 2001-2011. *Proc Sudd Oak Death Fifth Sci Symp*:3–11.

10. Valachovic Y, Lee C (2008) Wildland management of Phytophthora ramorum in northern California forests. *Proc Sudd Oak Death Third Sci Symp*:305–312.

11. Valachovic Y, Lee C, Twieg B, Rizzo D, Cobb R (2012) Suppression of Phytophthora ramorum Infestations through silvicultural treatment in California's north coast. *Proc Sudd Oak Death Fifth Sci Symp*:108–113.

1

Symbol	Meaning	Typical value	Source
τ_{it}	Epidemiological class of cell *i* in week *t*	S,C,I,D,T,R	Dynamic quantity
f_i	Forest type mask of cell *i*	R or M	Mapped as described in (1)
m_{it}	Moisture index in cell *i* in week *t*	0 – 1	Mapped as described in (1)
c_{it}	Temperature index in cell *i* in week *t*	0 – 1	Mapped as described in (1)
ψ_{it}	Mean maximum number of infections from site *i* in week *t*	$\beta\chi_t(f_i)m_{it}c_{it}i_{it}$	Dynamic quantity
β	Rate of infection	4.55 wk^{-1}	Recalibration of the model (see Fig. S3)
$\chi_t(f_i)$	Indicator controlling whether forest type in cell *i* is susceptible and infectious in week *t*	0 or 1	Mapped as described in (1)
$K(d;\alpha_1,\alpha_2,\gamma)$	Dispersal kernel	Equation (1)	Fitted to data as described in (1)
α_1	Scale parameter for short-range dispersal	20.57 m	Fitted to data as described in (1)

α_2	Scale parameter for long-range dispersal	9.504 km	Fitted to data as described in (1)
γ	Proportion of dispersal that is short-range	0.9947	Fitted to data as described in (1)
θ	Rate at which symptoms emerge	1/260 wk^{-1} (f_i = M) 1/156 wk^{-1}(f_i = R)	(5, 11)
ρ	Rate at which removed host units re-establish	0.2 yr^{-1}	(11)
p	Probability of detecting a symptomatic cell in a single survey	0.8	(4)
L	Control radius	375 m	Assumed (but is varied)
T	Year in which detection and control start	2002	Assumed (but is varied)
C	Constant additional budget for control in year *y*	50 km^2/yr	Assumed (but is varied)
C(y)	Variable additional budget for control in year *y*	$C(y) = C_0\alpha^{y-T}$	Assumed
α	Control decay factor	1	Budget does not change over time

C_0	Area that can be controlled in the first year when the amount of control varies over time	See calculation in main text	Calculated to ensure total budget does not depend on α
-	Strategy used to prioritize cells for control	No prioritization, with random selection of sites to treat	Assumed (but is varied)
σ_j	Weight of cell *j* in the detected list	A random number	Assumed (but is varied)
H_k	Hazard of cell *k*	Average number of cells infected following isolated introduction	Calculated (Fig. S2C)
Q	Radius of the neighborhood over which control weightings are averaged	2 km	Selected after initial scan

Table S1. Summary of all parameters used in the model, with symbols and default values.

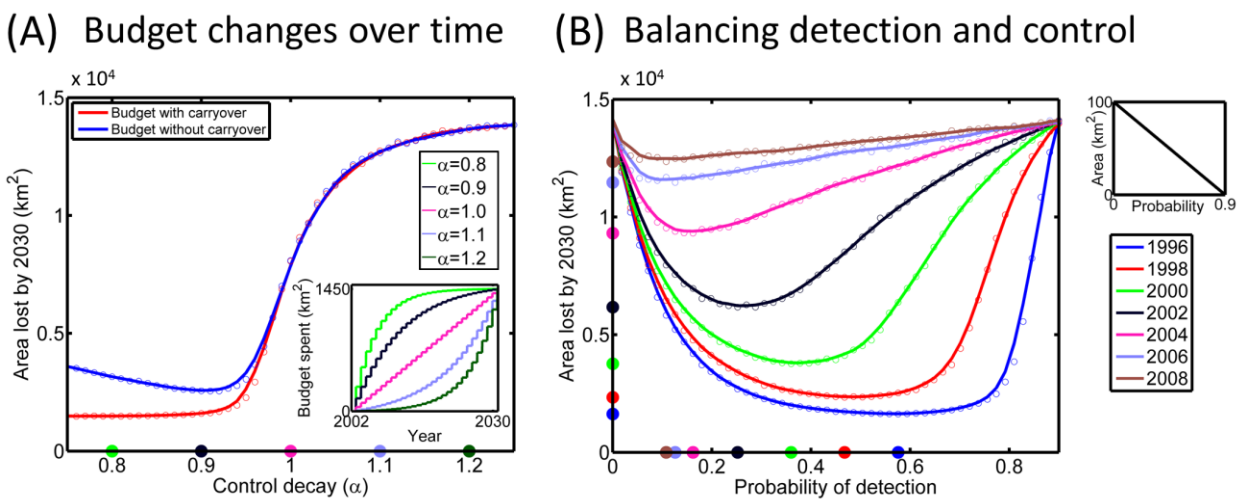

Fig. S1. Changing budgets over time, and balancing the costs of detection and treatment. (A) Response of the area lost by 2030 to the control decay factor, α, with and without carryover of any excess budget at the end of each year. The time-dependent total budget is shown for different values of α in the inset. In all cases the maximum that can be spent 2002 – 2030 is equivalent to a fixed budget allowing control of 50km^2/yr. (B) Response of the area lost by 2030 to the probability of detection, *p*, when there is a shared budget for detection and treatment. The linear trade-off between the probability of detection and the area that can be controlled per year (top right) means that each value of *p* corresponds to a certain yearly budget. Dots show the optimal detection probability and minimum median area lost for each year in which treatment starts. Here we assume the budget allows up to 100km^2/yr to be treated if it is all spent on control, and revert to the baseline control scenario (i.e. sites to treat are selected randomly from the set of sites known to contain detected infection, with a fixed control radius of 375m around infected sites).

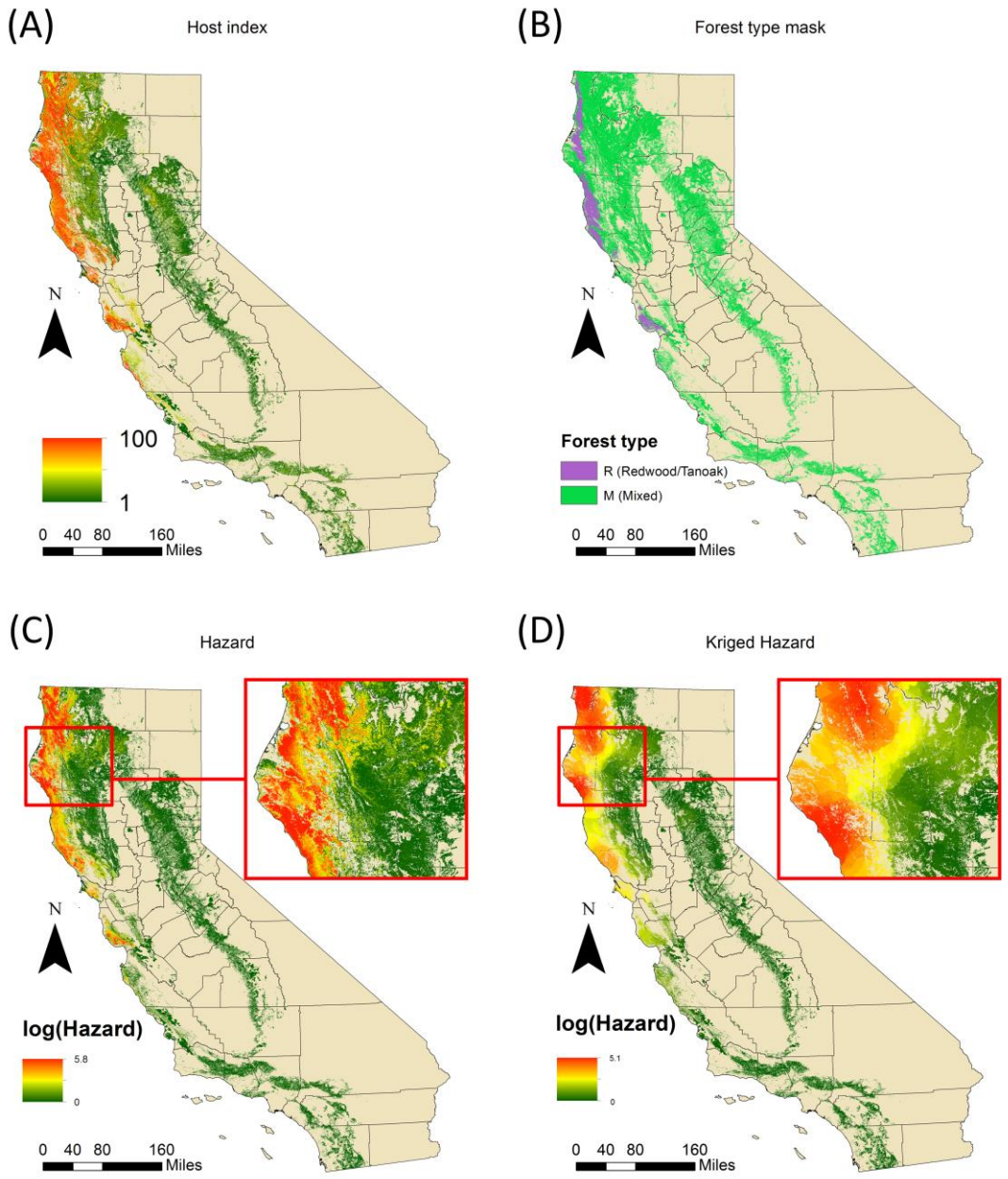

Fig. S2. Maps. (A) The host index. (B) The forest type mask. (C) The hazard map, calculated on a cell-by-cell basis. (D) The hazard map as presented in Meentemeyer *et al.* (1), calculated via spatial kriging of the hazard values from 1,000 randomly chosen locations. Comparing (C) and (D) shows significant small-scale detail was omitted from the previous version. Note the range of hazard values on the newer map is larger: this is because the random selection of 1,000 sites used to build the older version did not include certain sites with particularly high values of the hazard.

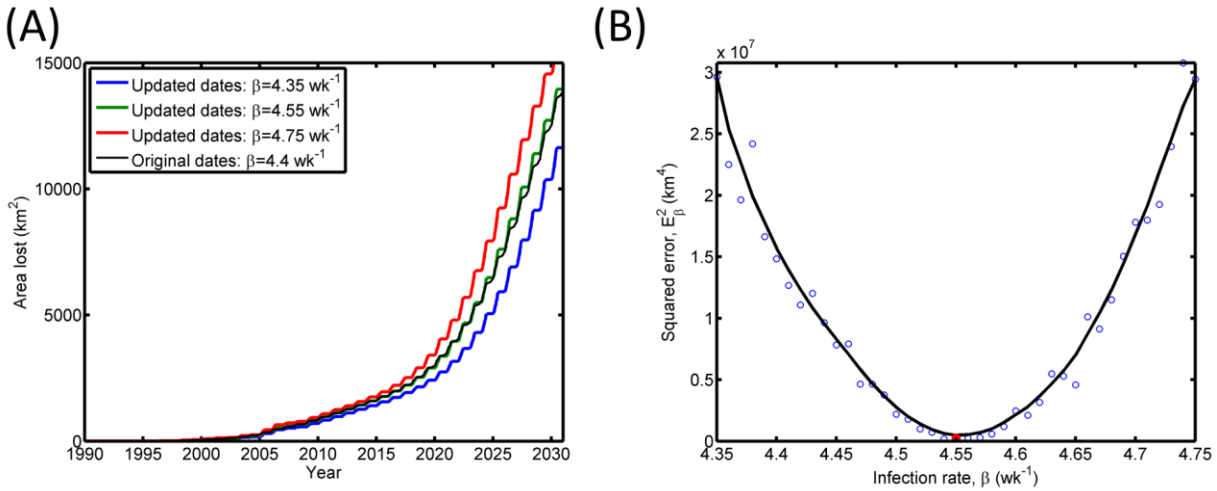

Fig. S3. Recalibration of the infection rate, β. (A) Area lost when there is no control as a function of time, comparing the median area infected over time in the model when using the originally-reported sporulation dates and the original infection rate $\beta = 4.4 wk^{-1}$ (the black curve), with the results using the updated sporulation dates and a number of different values of β. (B) The sum of squared differences between the disease progress curve from the model using the original date range and original value of β, and the disease progress curves in the model for a range of vales of β, E_{β}^{2} (see Equation (2)). The optimal value $\beta = 4.55 wk^{-1}$ is marked in red.

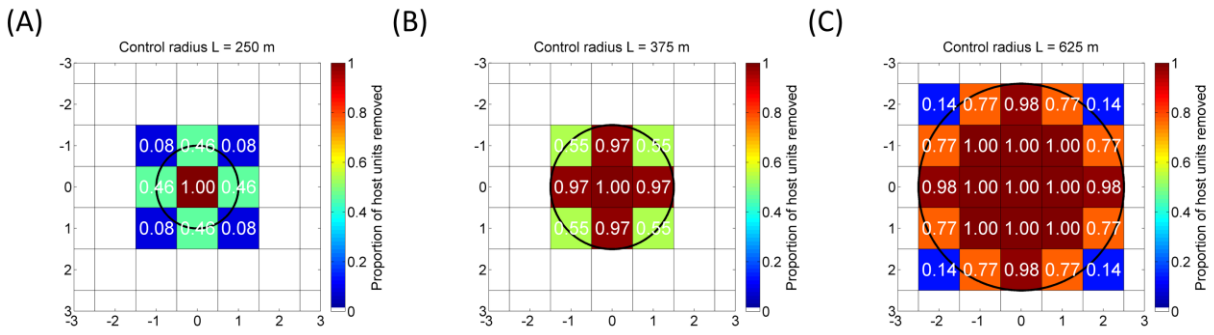

Fig. S4. Control Radius. Proportion of host removed in the neighborhood of a detected cell for different values of the control radius, *L*. (A) *L* = 250m, (B) *L* = 375m (default value), (C) *L* = 625m.

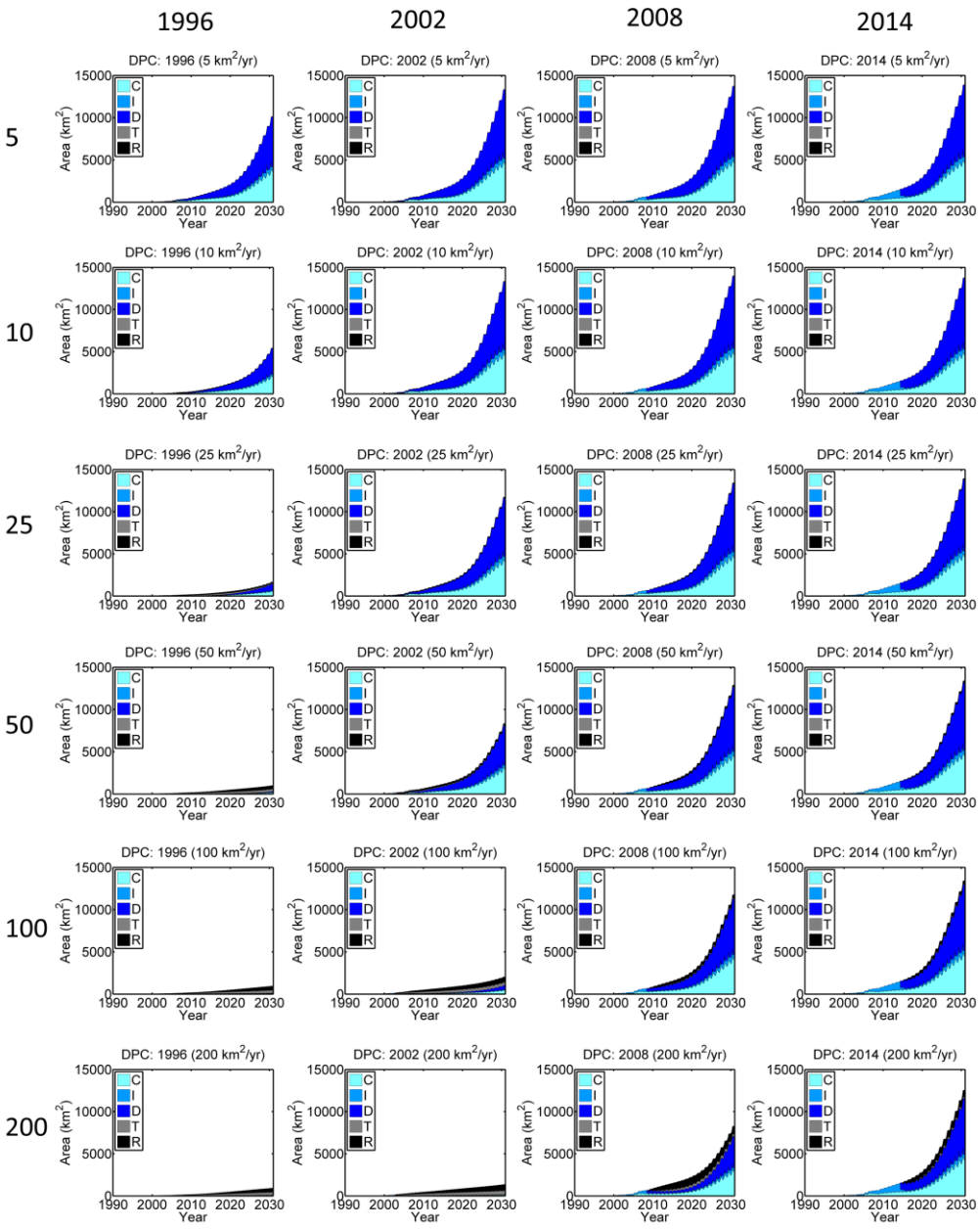

Fig. S5. Area lost over time. Disease progress curves for selected points on Fig. 3A in the main text, showing the average area in each non-susceptible compartment as a function of time, for control that starts in different years (1996 vs. 2002 vs. 2008 vs. 2014) and with different budgets available for control (5km^2/yr vs. 10km^2/yr vs. 25km^2/yr vs. 50km^2/yr vs. 100km^2/yr vs. 200km^2/yr). In all cases control selects sites for treatment at random from the list of sites known to contain uncontrolled infection, and removes host up to a control radius of 375m.

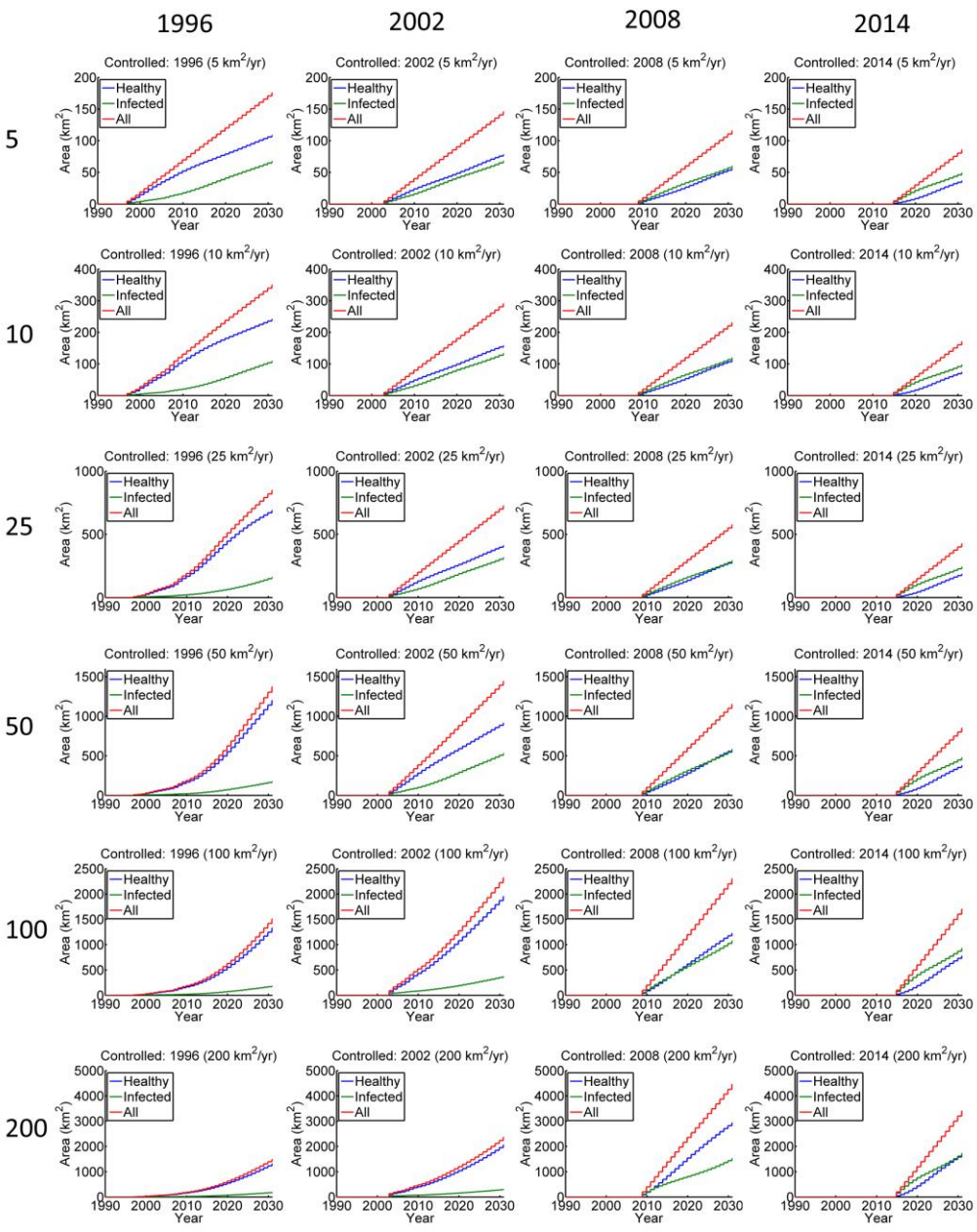

Fig. S6. Area controlled over time. Area of uninfected (blue), area of infected (green), and total area of host removed as a function of time for different years of starting control and control budgets (*cf.* Fig S5 for the corresponding disease progress curves). Note the scale of the y-axis is different on each row.

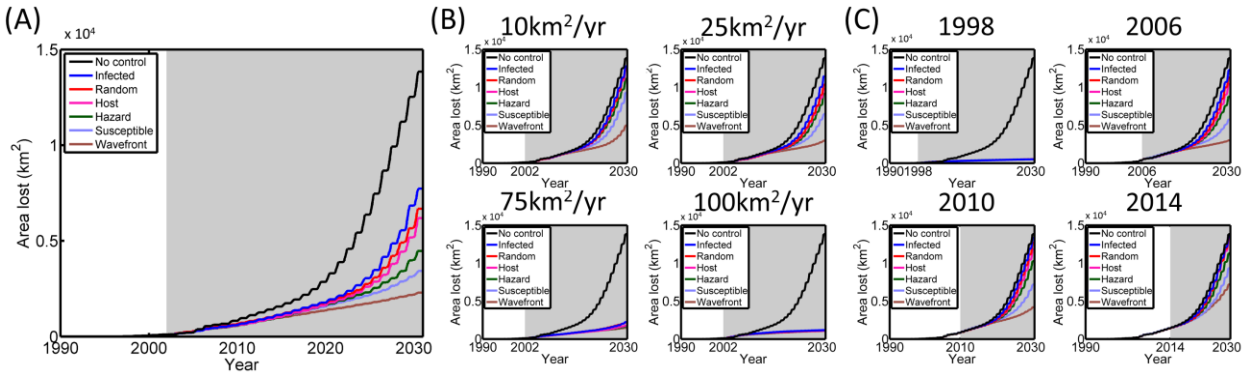

Fig. S7. Disease progress for different methods of selecting sites to treat. Average area lost over time for the different spatial strategies, using the optimal control radius obtained for each strategy (*cf*. Fig. 5 in the main text). (A) Control starting in 2002, with budget that allows up to 50km^2 to be controlled per year. (B) Control starting in 2002, with different budgets. (C) Control that allows up to 50km^2 to be controlled per year, with different starting years. In all figures, the period for which control of the epidemic is attempted is marked in grey.

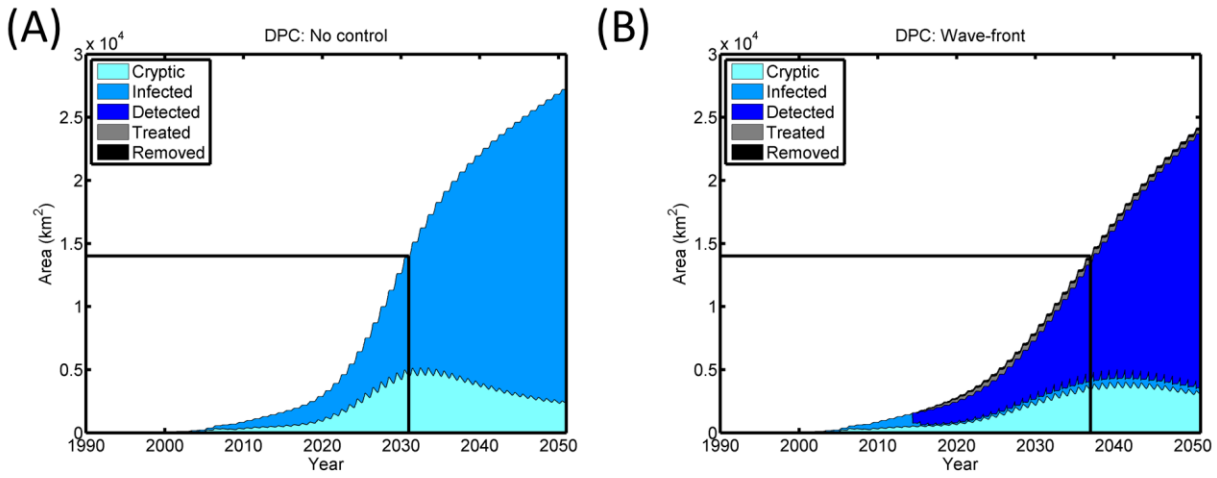

Fig. S8. The wave-front strategy starting 2014 only delays disease. (A) Disease progress over time when the epidemic is not controlled, making predictions until 2050. (B) Disease progress when the wave-front is targeted, starting in 2014 and continuing until 2050 (budget allows removal of up to 50km^2/yr). On both curves the time until an area of 14,000km^2 is lost is marked: controlling on the wave-front corresponds to a seven year delay in reaching the same area lost in comparison to not controlling at all.

(A) Status after a single round of detection

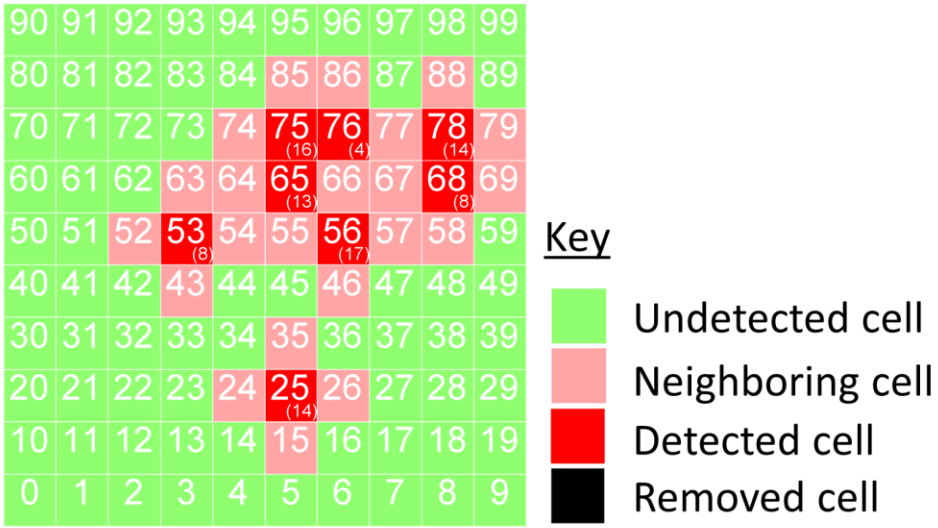

(B) Treat first (default)

j	N	E	S	W
$56_{(17)}$	66	57	46	55
$75_{(16)}$	85	76	65	74
$78_{(14)}$	88	79	68	77
$25_{(14)}$	35	26	15	24
$65_{(13)}$	75	66	55	64
$68_{(8)}$	78	69	58	67
$53_{(8)}$	63	54	43	52
$76_{(4)}$	86	77	66	75

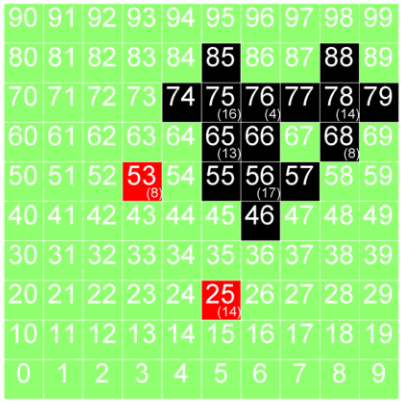

(C) Foci first

j	N	E	S	W
$56_{(17)}$	66	57	46	55
$75_{(16)}$	85	76	65	74
$78_{(14)}$	88	79	68	77
$25_{(14)}$	35	26	15	24
$65_{(13)}$	75	66	55	64
$68_{(8)}$	78	69	58	67
$53_{(8)}$	63	54	43	52
$76_{(4)}$	86	77	66	75

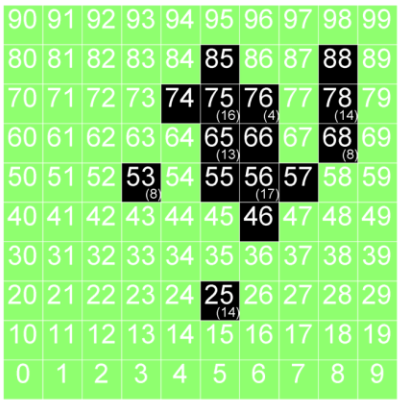

Fig. S9. Schematic illustrating "foci-first" control. (A) Schematic results of a round of detection: the larger number in white inside each cell is its cell id; the smaller number in detected cells is the cell's control priority, σ (here chosen at random for illustration). (B) The detected list and the set of sites that are eventually treated for the "treat first" control that is used by default, in which treatment is completed around each site before moving to the next element of the detected list. In the detected list, the index of each detected site (j) is shown, together with the indices of cells directly north, east, south and west are shown: we assume here for illustrative purposes that control completely removes all hosts in these neighboring cells. Black denotes cells that are controlled within a budget that allows 15 cells to be controlled. Gray shows cells that are controlled due to treatment caused by appearing in the control neighborhood of a cell somewhere higher up the list. On the schematic showing the status of the landscape after control, there are two detected foci that have not been treated, and so would possibly be treated next time. (C) As panel (B), but using the treat-first strategy, in which the central squares of each focus are treated first, then followed by the treatment out to a radius if there is remaining budget. Here this treats all detected cells, together with some neighbors of the detected cells with the higher control priorities.

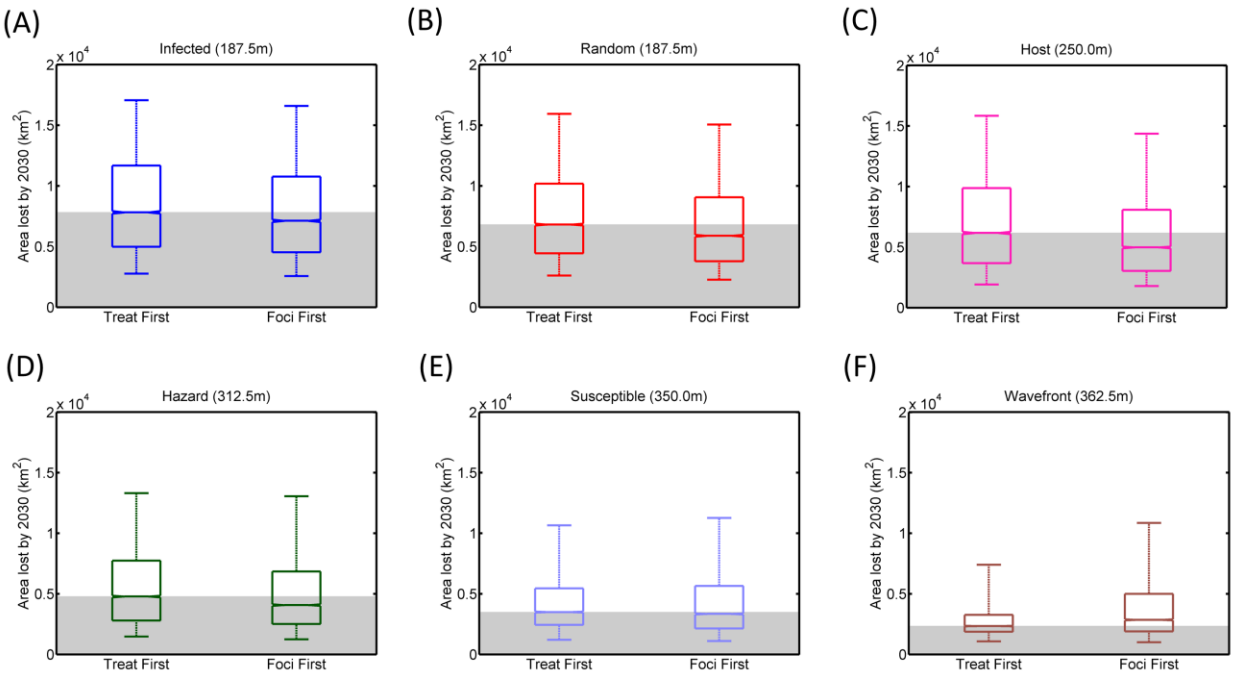

Fig. S10. Performance of "foci-first" control. Comparing "treat-first" (default) vs. "foci-first" control strategies, for each of the six methods of selecting sites to treat: (A) Infected, (B) Random, (C) Host, (D) Hazard, (E) Susceptible, (F) Wave-front. In all cases the control radius, *L*, is fixed at 375m, control starts in 2002, and there is sufficient budget to treat 50km^2/yr. The grey shading shows the median area lost when cells within the radius are treated first: our default treat-first strategy improves the performance of the wave-front strategy, has very little effect on the susceptible strategy, and makes the other four strategies perform slightly less well.

Legends for Movies

Movie 1. Baseline infection Risk. Risk of infection over time (1990-2030) when there is no control (*cf.* Figs. 1B and 1C in the main text).

Movie 2. High level of control starting 2014. Risk of infection or removal over time (1990-2030) when there is sufficient budget to allow control of up to 200km^2/yr starting in 2014 (random selection of sites for treatment from the detected list; control radius = 375.0m; *cf.* Figs. 2A – 2C in the main text).

Movie 3. Infected strategy starting 2002. Risk of infection or removal over time (1990-2030) when there is sufficient budget to allow control of up to 50km^2/yr starting in 2002 (preferentially treating sites from the detected list in areas where a large proportion of host is infected; optimized control radius = 187.5m; *cf.* Fig. 5A in the main text).

Movie 4. Random strategy starting 2002. Risk of infection or removal over time (1990-2030) when there is sufficient budget to allow control of up to 50km^2/yr starting in 2002 (random selection of sites for treatment from the detected list; optimized control radius = 187.5m; *cf.* Fig. 5A in the main text).

Movie 5. Host strategy starting 2002. Risk of infection or removal over time (1990-2030) when there is sufficient budget to allow control of up to 50km^2/yr starting in 2002 (preferentially treating sites from the detected list in areas where there is a large amount of *P. ramorum* host; optimized control radius = 250.0m; *cf.* Fig. 5A in the main text).

Movie 6. Hazard strategy starting 2002. Risk of infection or removal over time (1990-2030) when there is sufficient budget to allow control of up to 50km^2/yr starting in 2002 (preferentially treating sites from the detected list in areas in which there is predicted to be high local rates of spread due to high hazard [equivalent to high basic reproductive number]; optimized control radius = 312.5m; *cf.* Fig. 5A in the main text).

Movie 7. Susceptible strategy starting 2002. Risk of infection or removal over time (1990-2030) when there is sufficient budget to allow control of up to 50km^2/yr starting in 2002 (preferentially treating sites from the detected list in areas where a large proportion of host remains susceptible; optimized control radius = 350.0m; *cf.* Fig. 5A in the main text).

Movie 8. Wave-front strategy starting 2002. Risk of infection or removal over time (1990-2030) when there is sufficient budget to allow control of up to 50km^2/yr starting in 2002 (preferentially treating sites from the detected list at and ahead of the epidemic wave-front; optimized control radius = 362.5m; *cf.* Fig. 5A in the main text).